Scanning probe microscopy and potentiometry using a junction field effect transistor based sensor

Paul Graf, Meike Flebbe, Stephanie Hoepken, Detlef Utzat, Hermann Nienhaus, and Rolf Möller[a)]
Fakultät für Physik, Center for Nanointegration Duisburg-Essen (CENIDE), Universität Duisburg-Essen, Lotharstraße 1, 47057 Duisburg, Germany

(Received 31 August 2018; accepted 20 October 2018; published online 26 November 2018)

Scanning tunneling microscopy in its conventional form relies on a steady state tunneling current of 10^{-12}–10^{-6} A. However, for various applications, it is desirable to reduce the current load to a minimum. Here, we present first experiments using a cooled junction field effect transistor in open gate operation, thereby reducing the DC-current to less than 10^{-19} A. This enables almost ideal measurements of the local electrochemical potential on a surface. Various methods applying dynamic modes can be used to maintain a constant distance between the scanning probe and the sample surface. Here, we use an AC-bias applied to the sample and a lock-in amplifier connected to the preamplifier to evaluate the conductance of the tunneling gap. *Published by AIP Publishing.*
https://doi.org/10.1063/1.5054349

The field of scanning probe microscopy was strongly stimulated by the invention of scanning tunneling microscopy (STM) which enabled atomic resolution on a flat surface in real space for the first time.[1] Since then, various forms of scanning probe microscopes have been developed based on different interactions between the probe and the sample surface. Most prominent is scanning force microscopy using sensors which are able to detect the forces exerted on the scanning probe tip.[2] In the present paper, the possibilities of a junction field effect transistor (JFET) sensor providing an electrometer with almost infinite impedance will be discussed. It enables us to evaluate the local electrochemical potential μ_{EC} with a minimal current load on the sample surface which is well below the limit of conventional techniques.

Another STM related scheme is scanning tunneling potentiometry (STP), which was presented by Muralt and Pohl.[3] Thereby, it is possible to evaluate the local electrochemical potential at the position of the sample which faces the tip of a scanning tunneling microscope. The bias voltage at the sample is varied until the average tunneling current vanishes. The corresponding bias voltage corresponds to the local electrochemical potential. To enable scanning probe microscopy, the distance between the probe and the sample has to be controlled. Slightly different techniques were developed.[4–10] Most techniques rely on an additional alternating bias voltage, which leads to an AC-component of the tunneling current (I_{AC}) remaining at zero DC bias. Since it exhibits the same exponential distance dependence as the DC-tunneling current, it can be used to adjust the distance between the tip and the sample in analogy to conventional STM.

Recently, we have shown[11] that by using a conventional junction field effect transistor (JFET) at low temperature (<150 K), an electrometer with a resolution of 10 mV at a bandwidth of 10 kHz can be built, which has almost no static input current ($<10^{-19}$ A). Hence, this sensor is ideally suited to perform scanning tunneling potentiometry (STP) because it exerts no load on the source, and the influence of the probe on the electrochemical potential to be measured will be minimal.

For the experiment presented in this paper, the JFET (BF545 B) was combined with the tunneling tip of an ultra-high vacuum low temperature STM on a small carrier, which can be exchanged *in situ*. Figure 1 shows a schematic representation and a photo collage of the carrier and the sample.

Figure 2 displays the circuit diagram of the electrometer. The JFET is operated in an open-gate configuration, and only the tip of the STM is connected to the gate. The output of the JFET is connected to a current voltage converter with a gain of 10^4 V/A. The drain voltage is adjusted by R_1. The second op amp (OA2) subtracts the drain voltage. The gain of the open gate electrometer given by the transconductance of the particular JFET and the I-V converter is $dU_{out}/dU_{in} = 24$.

Since the gate of the JFET is formed by a pn-junction, there is no risk of harmful charging if no signal is applied. If

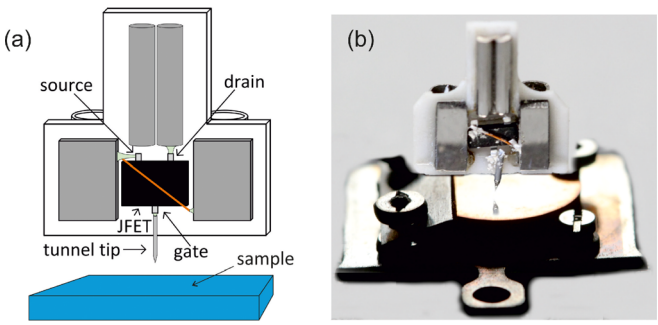

FIG. 1. (a) Schematic drawing of the experimental arrangement and (b) the photo composition of the JFET sensor for application in a low temperature scanning tunneling microscope. The metallic plates and rods connect the source and drain of the JFET sensor to the STM setup. The tunneling tip is directly connected to the gate of the JFET. Reprinted with permission from Graf *et al.* Rev. Sci. Instrum. **88**, 084702 (2017). Copyright AIP Publishing LLC 2017.

[a)]Author to whom correspondence should be addressed: rolf.moeller@uni-due.de

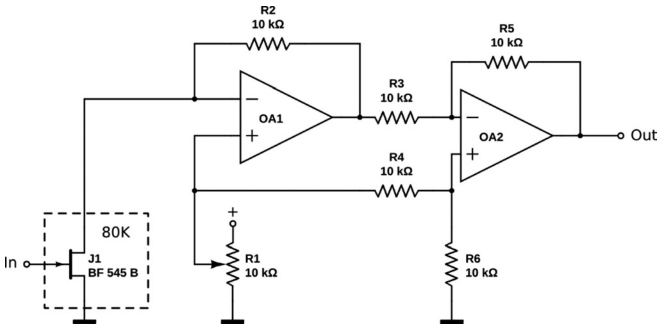

FIG. 2. Electric circuit of the open gate electrometer, reprinted with permission from Graf *et al*. Rev. Sci. Instrum. **88**, 084702 (2017). Copyright AIP Publishing LLC 2017.

the gate voltage is outside of the operating regime, either the forward or the Zener-current limits further charging of the gate. Hence, it is a robust configuration, and there is no need for protecting diodes, etc., connected to the gate. Since only the JFET itself has to be cooled, it may be easily combined with low temperature scanning probe microscopy (LT-SPM). The JFET can be placed at a position in the setup which resides at temperatures between 30 and 150 K. The dissipation by Joule heating is only about 1 mW.

For conventional STM, one cannot use the JFET-sensor because it is not possible to maintain a constant operational point of the JFET if a constant unidirectional current flows to the input of the open gate charge amplifier. Figure 3 shows the equivalent circuit for the combination of the sample, the tunneling barrier, and input of the JFET. The tunneling barrier given by the tip and the sample at a given distance exhibits a conductance of $S_{tunnel} \propto e^{-\alpha z}$ in parallel to a parasitic capacity C_{gap} given by the geometry of the tip and the sample which is on the order of 0.1 pF. z is the distance between the tip and the sample, and $\alpha \cong 2 \times 10^{10}\,\mathrm{m}^{-1}$ is the inverse decay length. The input of the JFET can be represented by a capacity C_{gate} of about 4 pF.

To evaluate the voltage at the gate V_{gate}, we consider the ratio r between the gate and the sample voltage

$$r = \frac{V_{gate}}{V_{sample}} = \frac{Z_{gate}}{Z_{gap} + Z_{gate}},$$

given by the impedance Z_{gate} of the gate of the JFET and the impedance Z_{gap} of the tunneling gap. To facilitate the calculation in the following, we use the conductance which is the inverse of the impedance and obtain

$$r = \frac{S_{gap}}{S_{gap} + S_{gate}}.$$

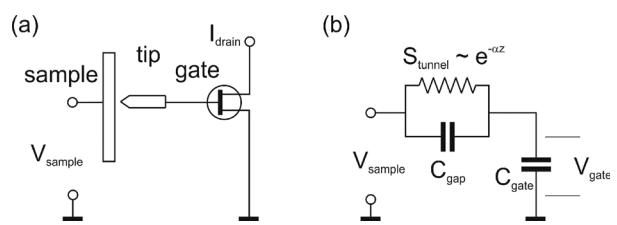

FIG. 3. (a) Schematic representation of the tunneling gap and the JFET sensor and (b) electric equivalent to (a). The tunneling junction can be described as a capacitance C_{gap} in parallel to the tunneling conductance S_{tunnel}.

The conductance of the tunneling gap is given by the sum of tunneling conductance and conductance due to the capacity of the tunneling gap

$$S_{gap} = S_{tunnel} + S_{gap\_capacity} = S_0 e^{-\alpha z} + i\omega C_{gap},$$

where $\omega = 2\pi f$ is the angular frequency of the AC sample voltage and $S_{gap\_capacity} = i\omega C_{gap}$ is the conductance of the gap capacity. Using $S_{gate} = i\omega C_{gate}$ for the conductance of the gate capacity of the JFET, the ratio r of the gate to sample voltage is finally given by

$$r = \frac{S_{tunnel} + i\omega C_{gap}}{S_{tunnel} + i\omega C_{gap} + i\omega C_{gate}} = \frac{S_{tunnel}^2 + \omega^2\left(C_{gap}^2 + C_{gap}C_{gate}\right) - iS_{tunnel}\omega C_{gate}}{S_{tunnel}^2 + \omega^2(C_{gap} + C_{gate})^2}.$$

Figure 4 displays the real part (dotted red line) and the imaginary part (dashed blue line) of r as a function of the tunneling conductance for a range of 0 to 100 nS (a) and 0 to 10 pS (b). For infinite conductance, the gate is directly connected to the sample, r approaches a value of 1, and the signal is in phase. For very low tunneling conductance, S_{tunnel}^2 may be neglected and we obtain

$$r = \frac{C_{gap}}{C_{gap} + C_{gate}} - iS_{tunnel}\frac{C_{gate}}{\omega(C_{gap} + C_{gate})^2}.$$

For vanishing conductance, the real part of r is constant, and the gate voltage is in phase with the sample voltage because the equivalent circuit is a capacitive voltage divider. However, the negative imaginary part starts linearly with the increasing tunneling conductance. If only the range up to 10 nS is used, there is no ambiguity, and the signal may be used for the feedback of the STM to maintain a constant distance between the probe and the sample. For the given parameters, it reaches a minimum at a conductivity of about $\sigma = 30$ nS. A stable operation of the feedback loop requires a monotonous function of the gap distance. Hence, only the range between 0 and of about $\sigma = 10$ nS should be used.

Figure 5 shows how the open gate electrometer is implemented in the circuit for scanning tunneling potentiometry. To apply a superposition $V_{sample} = V_{ext} + V_{mod}$ of a constant voltage and an ac modulation to the sample, the signal of the internal oscillator of the lock-in-amplifier is modulated onto the externally adjustable sample voltage. The operating point of the JFET is defined by $V_{ext} = -1.9\,V$, leading to an average source-drain current of 300 μA at a drain voltage of 2.8 V. To achieve stable tunneling, a modulation $V_{mod} = 0.05\,V_{rms}$ at 1.21 kHz is added. The output of the open gate electrometer is connected to the input of a lock-in-amplifier. The imaginary component measured –90° out of phase is fed into the feedback system and compared to a set value which is equivalent to 120 μV_{rms} at the gate of the JFET. From Fig. 4(b), we can evaluate that this corresponds to a tunneling conductance of 0.09 nS (a resistance of 11 GΩ) , which is low for normal STM operation and very low for scanning tunneling potentiometry.

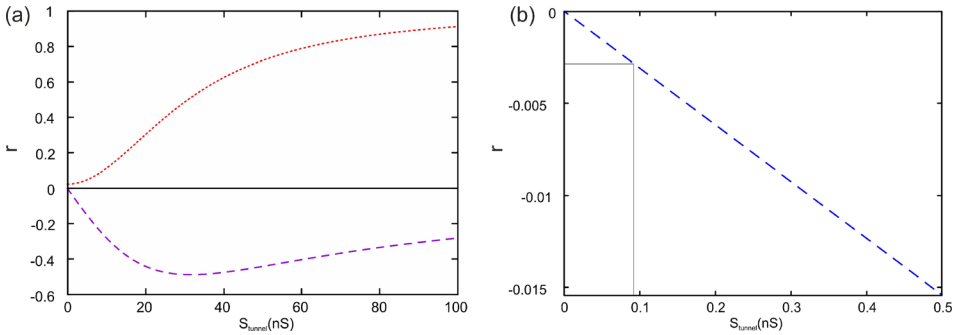

FIG. 4. Ratio of output voltage to AC sample bias as a function of tunneling conductance. The dotted red line displays the real part, and the dashed blue line displays the imaginary part (a) for the range of up to 100 nS and (b) for up to 0.5 nS.

Since the gate leakage current of the JFET is completely negligible, there is no net current between the tunneling tip and the sample, i.e., the tunneling current to and from the sample balance with a time constant $\tau_c = \frac{C_{gate}}{S_{tunnel}}$, which is typically on the order of a few milliseconds. Hence, the electrochemical potential of the tunneling tip becomes equal to the local electrochemical potential of the sample. The voltage at the tip is amplified by the open gate electrometer and measured at the output.

The local electrochemical potential may vary due a lateral current along the surface or as in our case due to a temperature difference. If the tip and the sample are at different temperatures and there is zero bias voltage, there would be a thermally driven current, which depends on the electronic density of states and the fermi distribution for the tip and the sample. In the case of zero external current, the tip will charge till the thermally driven current is matched by the tunneling current driven by the bias voltage. The latter is commonly referred to as "thermovoltage" of the tunneling barrier, see, e.g., Stoveng and Lipavsky.[12] It is this voltage which is measured in our experiment.

Prior to the experiment, a Cu(111) surface was prepared according to common practice by repeated cycles of sputtering with Ar^+ ions followed by annealing at 870 K. The tip which is attached to the JFET was cleaned by field emission *in situ* in the STM by placing it close to a sample surface and applying a voltage of around –250 V to drain and source of the JFET that leads to a forward current over the gate junction in the range up to 10 μA. A resistor of 10 MΩ was set in series to avoid excessive currents. After this procedure, the tip is sufficient clean to perform STM measurements.

Figure 6(a) shows that for an area of about $50 \times 40\,nm^2$, the topography of a Cu(111) surface was measured by operating the feedback loop for the tunneling distance as described above. The measurements have been performed at about 80 K. Flat terraces and a few atomic steps can be identified. It is obvious that a stable operation of the scanning probe microscope with a JFET sensor is possible. Figure 6(c)

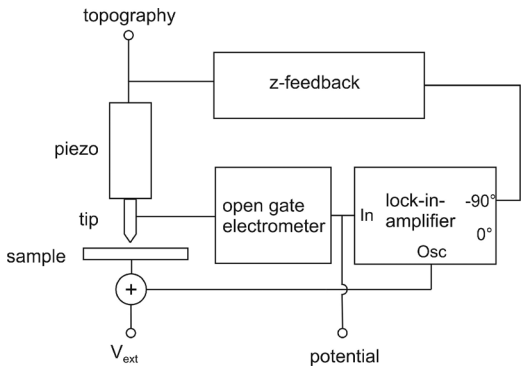

FIG. 5. Schematic representation of the experimental setup.

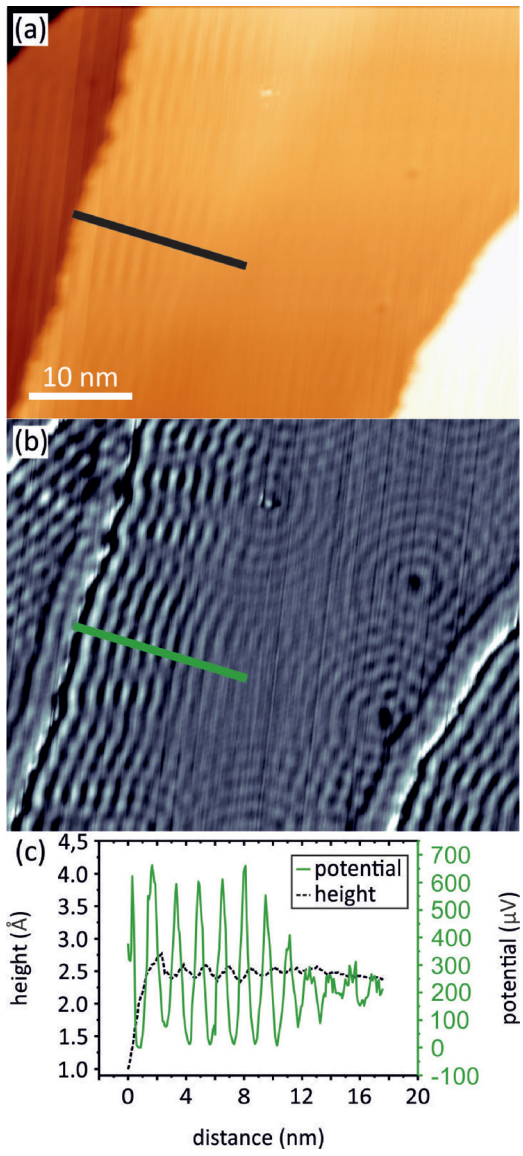

FIG. 6. Scanning tunneling microscopy and potentiometry of a Cu(111) surface at about 80 K. (a) displays the topography resulting from the feedback loop using the imaginary part of the AC gate voltage of the JFET sensor and (b) shows the DC part of the gate voltage which tracks the local electrochemical potential on the surface. A standing wave patterns is observed which is related to the Shockley type surface state at the Fermi energy; (c) shows line scans along the black and green lines displayed in (a) and (b), providing an estimate for the resolution; the black dotted line shows the topography, and the green continuous line shows the electrochemical potential.

displays a line scan (black dotted line), giving an estimate for the achieved resolution. It is limited by the stability of the instrument in the same way as conventional STM and by fluctuations introduced by the feedback loop for the distance. Similar to other schemes for scanning tunneling potentiometry, the bandwidth of the feedback is reduced compared to the standard STM feedback due to the more complicated feedback scheme using a lock in amplifier.

Since the gate voltage of the JFET follows the electrochemical potential of the sample, the output of the electrometer directly provides a signal proportional to μ_{EC} as long as the signal is small compared to the working range of the JFET which is about +/– 50 mV. Figure 6(b) displays the variation of the potential measured simultaneously to the topography. The line scan in Fig. 6(c) shows the resolution which is limited by the noise of the JFET.[11] Again, this is similar to the other techniques of scanning tunneling potentiometry using a current-to-voltage amplifier, which rely on a JFET at the input stage. Depending on the integration time, i.e., the scanning speed, a resolution of about 10 μV can be achieved at typical working parameters.

The potential displayed in Fig. 6(b) exhibits a modulation which clearly shows the characteristic features of standing electron waves due to the reflection of the electronic wave function at the step edges which are characteristic of the Cu(111) surface.[13] Since the potential of the probing tip and the sample is equal, the electronic surface state is probed at the Fermi energy. The Fermi wavelength is about 3 nm. In the present measurement, the absolute square of the wave function can be seen and hence half of the Fermi wavelength. From previous experiments, we know that the tip is at a higher temperature than the sample, leading to a thermovoltage at the tunneling gap. This has been observed experimentally for various situations.[9,14,15] The thermovoltage of the vacuum barrier has been described theoretically by Stovneng and Lipavsky.[12] According to their calculations, the observed variations are related to the derivative of the electronic density of states versus energy. This leads to a modulation of the signal which roughly scales with the square of the wave function. This is confirmed by the comparison of the line scans in Fig. 6(c). The thermovoltage although correlated with the local density of states is not in phase with the topography, which displays the modulation of the local density of states. Similar results have been published for the thermovoltage on Au(111), Ag(111), and Cu(111).[16,17]

The experiments presented in this paper show that an open gate circuit using a cooled JFET enables us to perform scanning probe microscopy at very low tunneling conductance. Hence, it may be applied to samples which exhibit a low conductivity. Moreover, it is ideally suited to perform scanning tunneling potentiometry because the technique provides a direct measurement of the local electrochemical potential at the sample surface. The ultimate high impedance will allow local to study, i.e., the photo- or chemovoltage of clusters, molecules, or nanoparticles. The method could be ideally combined with dynamic force microscopy, providing the feedback loop for the tip sample distance.

This work was supported by the Deutsche Forschungsgemeinschaft through SFB1242 "Non-equilibrium dynamics of condensed matter in the time domain."

[1]G. Binnig, H. Rohrer, C. Gerber, and E. Weibel, Phys. Rev. Lett. **49**, 57 (1982); in *Scanning Probe Microscopy*, edited by R. Wiesendanger (Springer, 2010).
[2]G. Binnig, C. Quate, and C. Gerber, Phys. Rev. Lett. **56**, 930 (1986).
[3]P. Muralt and D. Pohl, Appl. Phys. Lett. **48**(8), 514 (1986).
[4]J. R. Kirtley, S. Washburn, and M. J. Brady, Phys. Rev. Lett. **60**(15), 1546 (1988).
[5]J. P. Pelz and R. H. Koch, Rev. Sci. Instrum. **60**(3), 301 (1989).
[6]J. P. Pelz and R. H. Koch, Phys. Rev. B **41**(2), 1212 (1990).
[7]M. A. Schneider, M. Wenderoth, A. J. Heinrich, M. A. Rosentreter, and R. G. Ulbrich, Appl. Phys. Lett. **69**, 1327 (1996).
[8]B. G. Briner, R. M. Feenstra, T. P. Chin, and J. M. Woodall, Phys. Rev. B **54**(8), R5283 (1996).
[9]D. Hoffmann, A. Rettenberger, C. Baur, K. Läuger, J. Y. Grand, and R. Möller, Appl. Phys. Lett. **67**(9), 1217 (1995).
[10]A. P. Baddorf, "Scanning tunneling potentiometry: The power of STM applied to electrical transport," in *Scanning Probe Microscopy*, edited by S. Kalinin and A. Gruverman (Springer, Springer, New York, NY, 2007).
[11]P. Graf, M. Flebbe, D. Utzat, H. Nienhaus, and R. Möller, Rev. Sci. Instrum. **88**, 084702 (2017); patent pending.
[12]J. A. Stovneng and P. Lipavsky, Phys. Rev. B **42**(14), 9214 (1990).
[13]M. F. Crommie, C. P. Lutz, and D. M. Eigler, Nature **363**, 524 (1993).
[14]C. C. Williams and H. K. Wickramasinghe, Nature **344**(6264), 317 (1990).
[15]J. Park, G. He, R. M. Feenstra, and A.-P. Li, Nano Lett. **13**, 3269 (2013).
[16]D. Hoffmann, A. Rettenberger, K. Läuger, J. Y. Grand, and R. Möller, Phys. Rev. B **52**(19), 13796 (1995).
[17]K. J. Engel, M. Wenderoth, N. Quaas, T. C. G. Reusch, K. Sauthoff, and R. G. Ulbrich, Phys. Rev. B **63**, 165402 (2001).